140-Gbaud PAM-8 IM/DD Transmission and FTN Signal Processing based on Low-Complexity Nonlinear M-BCJR Equalization with Deep Neural-Network Channel Model

An Yan(1), Sizhe Xing(1), Guoqiang Li(1), Zhongya Li(1), Penghao Luo(1), Aolong Sun(1), Jianyang Shi(1), Hongguang Zhang(2), Xi Xiao(2,3,4), Zhixue He(4), Nan Chi(1,4), and Junwen Zhang(1,4)*

(1) Key Lab of EMW Information (MoE), Fudan University, Shanghai 200433, China,
(2) National Information Optoelectronics Innovation Center, CICT, Wuhan, China, 200433
(3) State Key Lab of Optical Communication Technologies and Networks, CICT, Wuhan, China, 200433
(4) Peng Cheng Lab, Shenzhen 518055, China, *junwenzhang@fudan.edu.cn

Abstract *We propose and experimentally demonstrate an FTN signal processing scheme based on low-complexity nonlinear M-BCJR equalization with DNN model for nonlinear channel fitting in IM/DD system, achieving 140-GBaud PAM-8 signal transmission over 0.5-km SSMF in the C-band and a net-data-rate of 340 Gbps/λ.*

Introduction

The growing demand for data traffic in datacenter interconnects (DCIs) is driven by the rapid spread of cloud and social media services. Applications such as social networking, video streaming, and the Internet of Things are primarily running on DCIs, with higher traffic demand for intra-DC interconnections (typically spanning < 2 km) compared to inter-DC ones [1]. While intensity modulation and direct detection (IM/DD) technology remains the dominant solution for 400-Gbps intra-DCI due to its cost-effectiveness and power efficiency, the next-generation Ethernet is expected to reach 800-Gbps or even 1.6-Tbps intra-DCI, requiring over 200-Gbps per lane to improve spectral efficiency, reduce bandwidth requirements, and simplify transceiver device implementation. Simple pulse amplitude modulation (PAM) with moderate digital signal processing (DSP) is the preferred option in such scenario, offering greater spectral efficiency and suitability for next-generation Ethernet.

Towards advanced modulation formats and higher baud rates, the signals will suffer from the non-linear transfer response of transceivers, power fading effects from chromatic dispersion and square-law detection of photodetectors, and the inter-symbol interference (ISI) caused by bandwidth limitations of the transceivers. Conventional feedforward equalization (FFE) is not effective in mitigating these issues. To address this challenge, faster-than-Nyquist (FTN) approaches, such as maximum likelihood sequence estimation (MLSE) [2-4] and maximum a posteriori probability (MAP) decoding [5-8], have been developed. Among them, MAP equalizer with high-quality soft output is more compatible with soft-decision forward error correction (SD-FEC) [5], thus more suitable for ultra-high baud-rate signal transmission. However, the conventional MAP equalizer employs a linear finite impulse response (FIR) filter to estimate the channel response and calculate the transition metric, which is not accurate enough in modelling the nonlinear transfer function in the actual system.

Therefore, in this paper, we adopt a deep neural network (DNN) instead of the FIR filter in the FTN-type BCJR equalizer, which can accurately estimate the channel response by considering both linear and nonlinear transfer functions. We combine a simple DNN estimator and simplified M-BCJR decoder, achieving a low-complexity nonlinear M-BCJR equalizer with high-quality soft output for SD-FEC. With this method, we experimentally demonstrate the transmission of a 140-GBaud PAM-4/6/8 signal in an IMDD system over 0.5-km standard single-mode fiber (SSMF) in C-band, achieving a net-data-rate of 340 Gbps/λ when PAM-8 is applied.

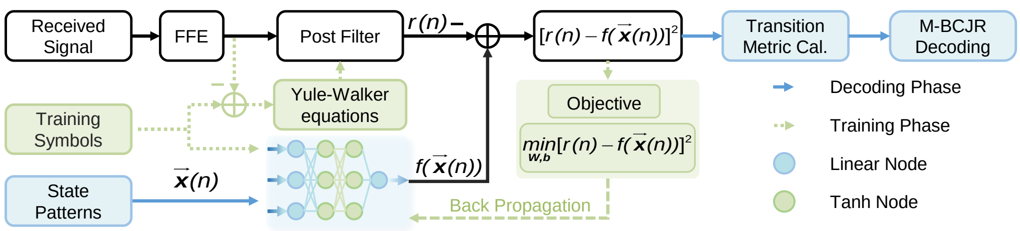

Fig. 1. The block diagram of the DNN-MBCJR equalization scheme, with DNN as the nonlinear channel response estimator and simplified MBCJR decoder for the reduction of overall complexity.

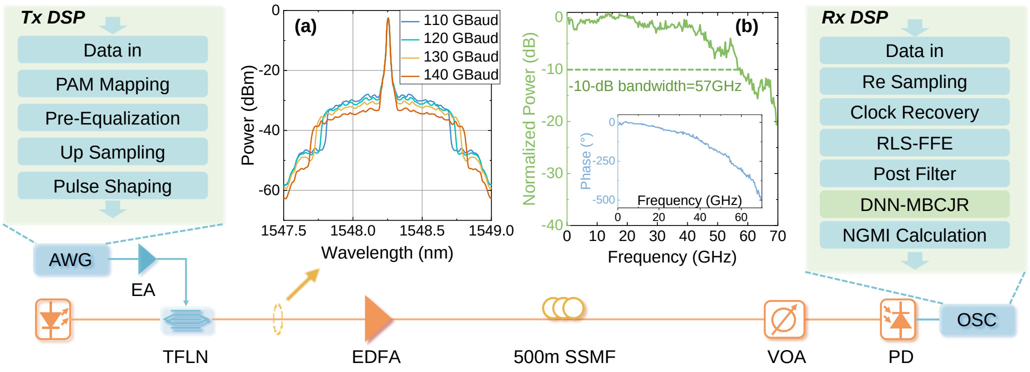

Fig. 2: Experiment setup for the ultra-high baud-rate PAM-8 IM/DD transmission over 0.5-km SSMF with the detailed DSP blocks. The inset (a) shows the measured optical spectra of PAM-8 signals for different baud-rates after electro-optical conversion, and the inset (b) represents the frequency response of overall system for B2B case.

Principle

In the bandwidth-constrained system, noise enhancement at high-frequency components is generally observed after applying linear adaptive equalizations. To improve the overall SNR performance of the system, a post filter (PF) is required, with the transfer function of $H(z) = 1 + \lambda z^{-1}$, and can be obtained based on Yule-Walker equations for the autoregressive coefficients extraction [9]. The filter located in the system introduces known ISI which must be eliminated by a post-equalizer, such as the BCJR decoder based on MAP rules. However, the conventional BCJR equalizer's performance is limited when nonlinear distortion exists. To overcome this limitation, we adopt a DNN-based nonlinear channel emulator to calculate the transition metric in our BCJR algorithm (referred to as DNN-M-BCJR), as illustrated in Fig. 1. A simple four-layer DNN is applied, with input layer, two hidden layers with the hyperbolic tangent function as the nonlinear function and an output layer with one linear fully-connected nodes. The number of nodes in input layer represents the memory length of state pattern each stage in the BCJR algorithm. And the output of DNN is used for the calculation of transition metric needed in BCJR decoder, which can be expressed as:

$$\Gamma = \frac{P(x')}{\sqrt{\pi N_0}} \exp\left[-\frac{\left[r(n) - f\left(\vec{x}(n)\right)\right]^2}{N_0}\right] \qquad (1)$$

Where $P(x')$ is the prior probability of the symbol that causes the transitions, N_0 is the noise variance, $r(n)$ is the output of the post filter at stage-*n* and $f\left(\vec{x}(n)\right)$ is the output of the DNN with state pattern $\vec{x}(n)$ as the input. Before the decoding phase, DNN is pre-trained by utilizing the training sequence as inputs and minimizing the mean squared error between the output of the DNN and the received signal processed by FFE and the post filter via back propagation.

Considering that the conventional BCJR equalization method is complicated due to the exponential increase in the number of states (X^L) with high-order modulation X or large pattern memory length L, we exploit a simplified BCJR decoder (named M-BCJR [10]) for the complexity reduction, which limits the number of states (X^L) to a fixed number M by discarding non-significant states with low probabilities at each trellis stage.

Experimental setup and results analysis

The experimental setup is depicted in Fig. 2. At the transmitter side, a PRBS is generated and then mapped to PAM-x symbols. Raised-cosine pulse-shaping and a linear pre-equalization is employed at Tx-side DSP. To drive the Mach–Zehnder modulator (MZM), the electrical signal is first amplified by an Electrical Amplifier (GT-LNA). Then, the continuous-wave light generated with a power of 10 dBm by an external cavity laser (ECL) at 1548 nm, is fed into the thin-film lithium niobate (TFLN, NOEIC MZ135-LN60) modulator with 3-dB bandwidth of 60 GHz. The optical signal, following its modulation, is transmitted over a 0.5-km SSMF and amplified by an Erbium-doped

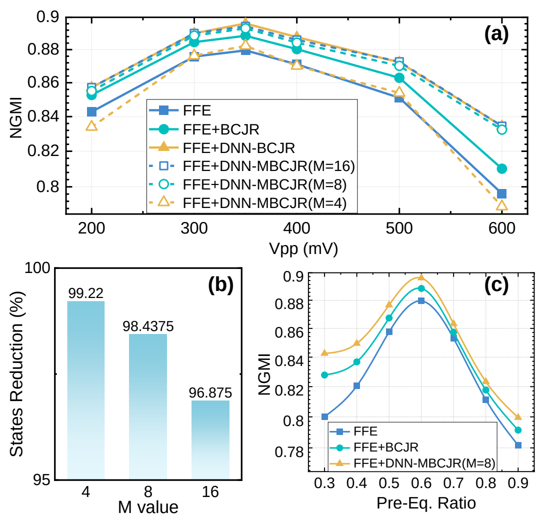

Fig. 3: The NGMI versus (a) the Vpp and (c) the pre-equalization ratio for a 140GBaud PAM-8 signal in B2B case. (b) is the percentage of states reduction for DNN-MBCJR algorithm with different M value

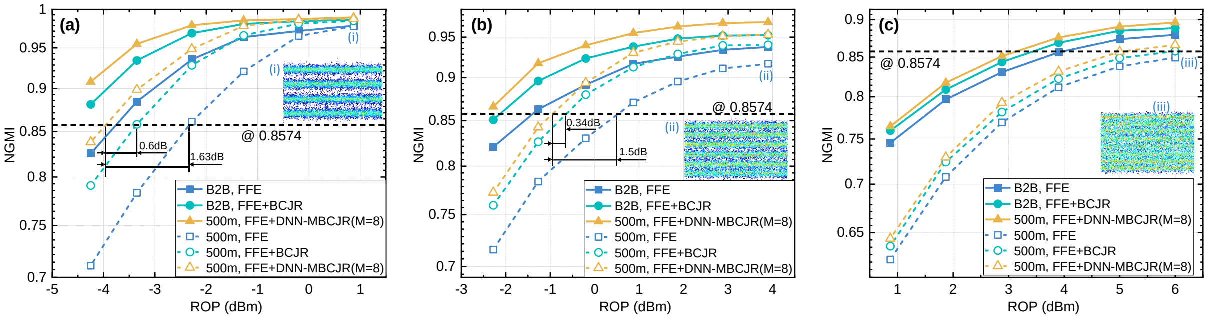

Fig. 4 The NGMI versus ROP for (a) 140-GBaud PAM-4, (b) 140-GBaud PAM-6 and (c) 140-GBaud PAM-8

Fiber Amplifier (EDFA). The current signal from the photodetector (PD, XPDV3320R), without any amplification from a trans-impedance amplifier, is sampled directly by an oscilloscope (OSC, Keysight UXR) with a sample rate of 256-GSa/s for subsequent offline digital signal processing. Shown in Fig. 2 (b), the system exhibits a -10-dB bandwidth of 57-GHz, which is sufficient for the transmission of a 140-Gbaud PAM signal through the use of nonlinear FTN-type M-BCJR equalization. In the offline Rx DSP, the signal is resampled to two samples per symbol (sps). Then the FFE takes the input at 2 sps and downconvert it to 1 sps for the subsequent nonlinear BCJR equalization. Finally, the DNN-M-BCJR algorithm with a memory length of $L = 3$ is applied to obtain the log-likelihood ratio (LLR) for the normalized general mutual information (NGMI) calculation [11].

Fig. 3 (a) shows the performance achieved at various peak-to-peak voltages (Vpp) values with 140-Gbaud PAM-8 at the back-to-back (B2B) case. As Vpp increases, the DNN-BCJR equalization outperforms conventional BCJR and FFE consistently, due to the superior ability of the DNN in nonlinear channel modelling. Additionally, DNN-M-BCJR exhibits comparable performance to the full-state DNN-BCJR with suitable M value ($M \geq 8$). However, the NGMI performance degrades a lot when it turns to a small M value (M=4) because it causes the mismatch between α and βsurvivors and thus produces some empty posterior probability. To strike a balance between NGMI performance and complexity, we set M= 8

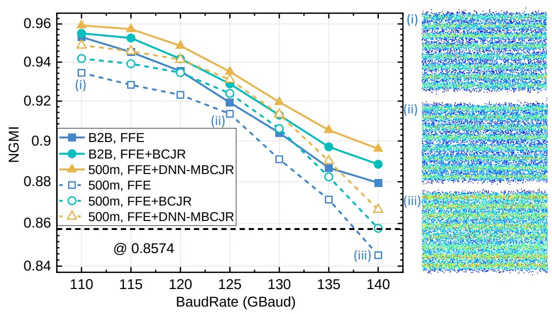

Fig. 5: The NGMI versus the baud-rate for a 140-GBaud PAM-8 signal at 6-dBm ROP

in the following discussions, yielding a state reduction of 98.43%. Fig. 3 (c) shows the relationship between NGMI and the pre-equalization ratio. The optimal pre-equalization ratio must be carefully selected, as a high ratio can lead to significant signal power loss and consequent degradation in SNR. In this case, a optimal pre-equalization ratio of 0.6 is used.

The sensitivity of 140-Gbaud PAM-x signals is presented in Fig. 4. To evaluate the system performance, a practical SD-FEC coding scheme is adopted, where a spatially coupled low-density parity-check code (with an inner code rate of 0.8167) is concatenated with an outer hard-decision BCH code [12]. This coding scheme achieves an overall rate of 0.8098 and an NGMI threshold of 0.8574. Results indicate that the DNN-M-BCJR equalization outperforms linear BCJR and FFE schemes, exhibiting power gains of 0.6 dB and 1.63 dB for PAM-4, 0.34 dB and 1.5 dB for PAM-6, and 0.3 dB and 0.75 dB for PAM-8, respectively, at the assumed NGMI threshold. This highlights the superior improvement in NGMI performance of DNN-M-BCJR in a bandwidth-limited system with nonlinear distortion.

Finally, we present the NGMI performance results for PAM-8 signals at different baud rates in Fig. 5. The DNN-M-BCJR scheme outperforms the conventional BCJR method in terms of LLR quality, and achieves the transmission of a 140-GBaud PAM-8 signal (net 340 Gbps) over 0.5-km SSMF, above the NGMI threshold assuming overall code rate of 0.8098.

Conclusions

We introduce a novel, computationally efficient DNN-M-CBJR technique and demonstrate its superior performance in comparison to traditional BCJR in a practical IM/DD system with nonlinear distortion. The experimental results reveal a successful transmission of net 340-Gbps PAM-8 signal over 0.5-km SSMF in the C-band.

Acknowledgements

This work was partly support by the NSFC project (No. 62171137, No. 62235005, No.61925104) Shanghai NSF project (No. 21ZR1408700) and The Major Key Project of PCL.

References

[1] X. Zhou, R. Urata, and H. Liu, “Beyond 1 Tb/s Intra-Data Center Interconnect Technology: IM-DD OR Coherent?,” Journal of Lightwave Technology, vol. 38, no. 2, pp. 475–484, Jan. 2020, doi: 10.1109/JLT.2019.2956779.

[2] D. Marsella, M. Secondini, and E. Forestieri, “Maximum Likelihood Sequence Detection for Mitigating Nonlinear Effects,” Journal of Lightwave Technology, vol. 32, no. 5, pp. 908–916, Mar. 2014, doi: 10.1109/JLT.2013.2294457.

[3] S. Yamamoto, H. Taniguchi, A. Masuda, M. Nakamura, and Y. Kisaka, “Evaluation of NGMI in 128-Gbuad PAM4 O-Band 10-km Transmission Using MLSE Based on Nonlinear Channel Estimation and Decision Feedback,” in 2022 European Conference on Optical Communication (ECOC), Sep. 2022, pp. 1–4.

[4] H. Taniguchi, S. Yamamoto, A. Masuda, Y. Kisaka, and S. Kanazawa, “800-Gbps PAM-4 2-km Transmission using 4-λ LAN-WDMTOSA with MLSE based on Deep Neural Network,” in Optical Fiber Communication Conference (OFC) 2022, San Diego, California: Optica Publishing Group, 2022, p. Th2A.25. doi: 10.1364/OFC.2022.Th2A.25.

[5] D. Che and X. Chen, “Higher-Order Modulation vs Faster-Than-Nyquist PAM-4 for Datacenter IM-DD Optics: An AIR Comparison Under Practical Bandwidth Limits,” J. Lightwave Technol., vol. 40, no. 10, pp. 3347–3357, May 2022, doi: 10.1109/JLT.2022.3172247.

[6] D. Che, “Ultra-Low-Complexity MAP Demapper for Bandwidth-Limited Pluggable Coherent Optics beyond 800G,” in Optical Fiber Communication Conference (OFC) 2022, San Diego, California: Optica Publishing Group, 2022, p. Th2A.33. doi: 10.1364/OFC.2022.Th2A.33.

[7] D. Che and X. Chen, “Faster-Than-Nyquist Signaling up to 300-GBd PAM-4 and 570-GBd OOK Suitable for Co-Packaged Optics,” in 2021 European Conference on Optical Communication (ECOC), Bordeaux, France: IEEE, Sep. 2021, pp. 1–4. doi: 10.1109/ECOC52684.2021.9606001.

[8] R. Rios-Müller, J. M. Estarán, and J. Renaudier, “Experimental estimation of optical nonlinear memory channel conditional distribution using deep neural networks,” in Optical Fiber Communication Conference, Los Angeles, California: OSA, 2017, p. W2A.51. doi: 10.1364/OFC.2017.W2A.51.

[9] L. Liu, L. Li, and Y. Lu, “Detection of 56GBaud PDM-QPSK generated by commercial CMOS DAC with 11GHz analog bandwidth,” in 2014 The European Conference on Optical Communication (ECOC), Cannes, France: IEEE, Sep. 2014, pp. 1–3. doi: 10.1109/ECOC.2014.6963961.

[10] A. Prlja and J. B. Anderson, “Reduced-Complexity Receivers for Strongly Narrowband Intersymbol Interference Introduced by Faster-than-Nyquist Signaling,” IEEE Trans. Commun., vol. 60, no. 9, pp. 2591–2601, Sep. 2012, doi: 10.1109/TCOMM.2012.070912.110296.

[11] A. Alvarado, E. Agrell, D. Lavery, R. Maher, and P. Bayvel, “Replacing the Soft-Decision FEC Limit Paradigm in the Design of Optical Communication Systems,” Journal of Lightwave Technology, vol. 33, no. 20, pp. 4338–4352, Oct. 2015, doi: 10.1109/JLT.2015.2450537.

[12] Q. Hu et al., “Ultrahigh-Net-Bitrate 363 Gbit/s PAM-8 and 279 Gbit/s Polybinary Optical Transmission Using Plasmonic Mach-Zehnder Modulator,” J. Lightwave Technol., vol. 40, no. 10, pp. 3338–3346, May 2022, doi: 10.1109/JLT.2022.3172246.